EFFECTS OF HIGH-ENERGY BALL MILLING PARAMETERS ON STRUCTURE AND THERMAL BEHAVIOR OF TINCAL

Tuğba TUNÇ PARLAK*, Neşe GÜÇLÜ KALEİÇLİ, Kenan YILDIZ
Sakarya University, Metallurgy and Materials Engineering, Esentepe Campus, 54187, Sakarya-TURKEY
ttunc@sakarya.edu.tr

Abstract: Tincal is widely used mineral in ceramic and metallurgy industries and raw material of borax production. It contains clay minerals and crystal water in the structure. Tincal, named as sodium tetraborate decahydrate, that has same formulation with borax, as known as borax decahydrate is the member of sodium borates and its formulation is expressed as $Na_2B_4O_7.10H_2O$ or $Na_2(B_4O_5(OH)_4).8H_2O$. Extra weight of water in raw boron minerals may become problem in point of transportation, storage, energy cost for producing anhydrous borates and by-product. In this study, with the aim of removing structural water and creating structural alterations for the forward mineral processing with less cost. High-energy ball milling, as known as mechanical activation process, was applied by planetary mono mill with variable parameters such as revolution per minute-speed of main disc (100, 200, 300, 400, 500 and 600 rpm for 30 min at ball-to-mass ratio 20), ball-to-mass ratio (10, 20, 30 and 40 for 30 min at 600 rpm) and mechanical activation time (15, 30, 60, 90 and 120 min). Investigations of effects of activations parameters were done by using X-ray diffraction analysis, Fourier transform infrared spectroscopy and thermal analysis. It was concluded that structure of tincal was changed and loss of crystalline water was occurred during high-energy ball milling.
Keywords: Tincal, Amorphization, Stress energy, Mechanical activation

Introduction

Boron compounds are used in many sectors such as glass, glass fibre, ceramic, hygienic and cleaning products, flame retarder, metallurgy-materials area, health, cosmetic and energy. Among all chemical elements, boron has the highest volumetric heat of combustion (140 kJ/cm^3) and the third highest gravimetric heat of combustion (59 kJ/cm^3) after H_2 and Be (Liu et al., 2014).

Boron minerals can be grouped as sodium borates, calcium borates, calcium borosilicate, magnesium borates and sodium-calcium borates. West Turkey possesses the largest boron deposits with a worldwide share of 72% (851 Mtons) in terms of B_2O_3 content, and controlled by the national mining enterprise Eti Mine (Kavas et al., 2011). Eti Mine has four production facility position. Kırka boron plant mainly works on borax and tincal. Colemanite and boric acid are products of Emet. Colemanite ($2CaO.3B_2O_3.5H_2O$) and ulexite ($Na_2O.2CaO.5B_2O_3.16H_2O$) are obtained via open pit mining at Bigadiç. Bandırma boron plant has a wide variety of boron products.

Tincal that has clay minerals in the structure is raw material of borax production. Borax from tincal is produced via batch process. Tincal is fed to a stirred reactor containing water heated to 95-100°C. Colloidal clay in the water is coagulate with an anionic coagulant. After coagulating and precipitating of clay, clear solution is passed to filter-pressing and is then fed to a crystallizer (Boncukoğlu et al., 1999).

Tincal that has same formulation with borax as known as borax decahydrate is the member of sodium borates. Its formulation is expressed as $Na_2B_4O_7.10H_2O$ or $Na_2(B_4O_5(OH)_4).8H_2O$. In this structure two molecules of water are structurally incorporated in the borate ion ($B_4O_5(OH)_4^{2-}$) as hydroxyl groups whereas remaining water molecules are present at outside of the ionic structure (Koçakuşak et al., 1995). Same situation is expressed for borax pentahydrate ($Na_2B_4O_7.5H_2O$) and stated that 3 mol of water of crystallization could be eliminated easily by thermal treatment but remaining 2 mol of water are strongly attached to the structure and can be removed by molecular decomposition (Sahin and Bulutcu, 2002). In many point, water in the structure may become problem such as transportation, storage and by-product.

Mechanical activation process or high energy milling has been using in the powder preparation area with the aim of synthesis of amorphous alloy powders or synthesis of alloy powders with other meta stable phases, synthesis of nanocrystalline powders, nanopowders, metal-ceramic composites and nanocomposite powders (Zhang, 2004). The fundamental principle of size reduction is supplied energy from grinding media to the powder. Trapping powder between two colliding balls compressed into small pieces (Alves et al., 2013).

In this study, with the aim of removing structural water and creating structural alterations for the forward mineral processing with less cost. High-energy ball milling, as known as mechanical activation process, was applied by planetary mono mill with variable parameters.

Materials and Methods

Tincal was obtained from Eti Mine, Bandırma/Turkey. Because of the decomposition of tincal occurs above 50°C, obtained material was dried at room temperature for one day to eliminate the dehydration of the structure. After drying, ore was milled and sieved under 75 µm for standardization to mechanical activation process.

The ore was mechanically activated in Planetary Mono Mill, Fritsch Pulverisette 6. Milling process was carried out under dry condition in tungsten carbide bowl that has 250 ml capacity with same material ball with 8.15 g in weight and 10 mm in diameter. Initially revolution per minute was tried at 100, 200, 300, 400, 500 and 600 rpm for 30 min at ball-to-mass ratio 20. After determining the efficiency of revolution, ball-to mass ratio studies were carried out at 10, 20, 30 and 40 for 30 min at 600rpm. After confirmation of revolution and ball-to mass ratio, mechanical activation durations were tried for 15, 30, 60, 90 and 120 min.

Mechanically activated samples were analysed by X-ray diffractometer to observe the structural alterations and amorphization degrees (*A*) were calculated by using Equation 1 (Baláž, 2008),

$$A = \left(1 - \frac{I_X . B_0}{I_0 . B_X}\right) . 100 \quad (1)$$

where I_0 is the integral intensity of the diffraction peak for the non-activated tincal, B_0 is the background of the diffraction peak for the non-activated tincal, and I_x and B_x are the equivalent values for the activated tincal (Baláž, 2008).

Also stress energy that is generated by mechanical activation process on the powder samples was calculated according to Equation 2 (Erdemoğlu et al., 2009).

$$SE\ (J/kg) = \frac{m_B}{m_S} . a . n . t_m . D \quad (2)$$

where m_B, m_S, a, n, t_M and D refer to mass of grinding media (kg), mass of material charge (kg), theoretical acceleration in the centre of the bowl in the planetary mill (m/s^2), speed of revolution (1/s), grinding time (s) and mill diameter (m), respectively. Theoretical acceleration for this planetary ball mill is 26.41 m/s^2, as stated by the supplier.

Fourier transform infrared spectroscopy to understand which changes in progress for bonds and thermal analysis to determine the decomposition temperature changes in the activated tincal were carried out. X-ray diffraction analysis was performed using a Rigaku Ultima X-ray diffractometer and Cu Kα radiation. FT-IR was done by Shimadzu between 4000 cm^{-1}-500 cm^{-1}. DTA was performed using TA Instruments SDTQ 600 at heating rate of 5°C.min^{-1} under atmospheric conditions.

Result and Discussion

XRD analysis of the sample was given in Figure 1. Borax (JPDS card no 01-075-1078), dolomite (JPDS card no 01-075-1656) and borax pentahydrate known as tincalconite (JPDS card no 01-071-1536) phases were detected. Peak overlapping phenomenon observed mainly between borax and tincalconite.

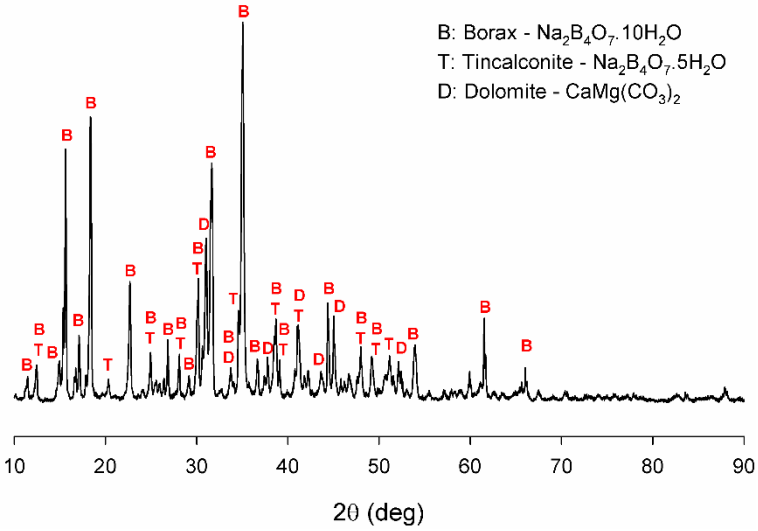

Figure 1. XRD analysis of the sample

Speed of main disc -revolution per minute- studies were carried out for 30 min and ball-to-mass ratio at 20. For observing changes at patterns, XRD was given at Figure 2 which was given between 10° - 40° to include most intensive peaks of the phases. At Figure 3, stress energy-I/I_0 (peak rate) and stress energy-amorphization degree (A%) dependence was given according to speed of main disc. As seen from the Figure 2, until 300 rpm no significant changes were obtained in terms of borax and dolomite. After 300 rpm, appearance of tincalconite was detected to accompaniment of intensity decrement of borax. By taking into consideration of crystallite size effect occurred as stretch and/or decrease in intensity of peak, peak rate (I/I_0) for borax presents at ~35° was considered where I_0 is the intensity of the non-activated sample and I is the intensity of activated one. As seen from the Figure 3, with increasing speed of main disc, stress energy increased. Peak rate decreased parallelly to amorphization degree increment. But these changes occurred drastically after 200 rpm in furtherance to XRD analysis. At higher speeds, due to temperature increase originated from ball-mass-bowl friction, borax phase underwent decomposition and in situ phase transformation to tincalconite occurred. When amorphization percentages were considered, speed of main disc was fixed at 600 rpm that borax patterns lost substantially.

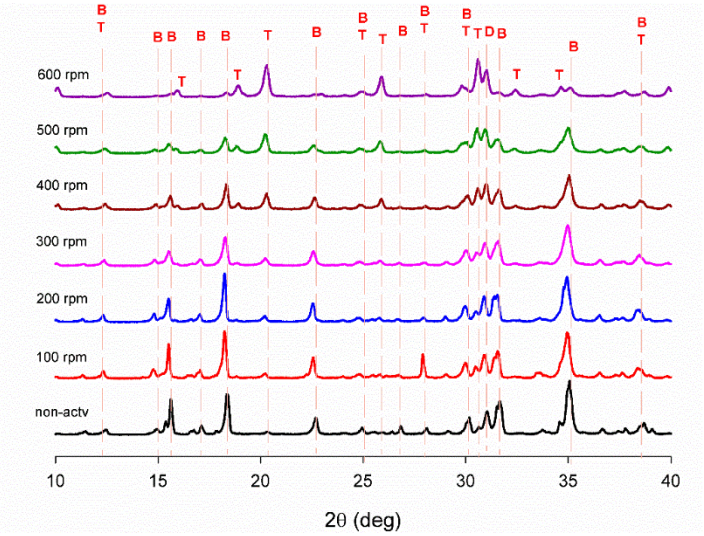

Figure 2. X-ray diffraction analysis of mechanically activated tincal sample at various speed

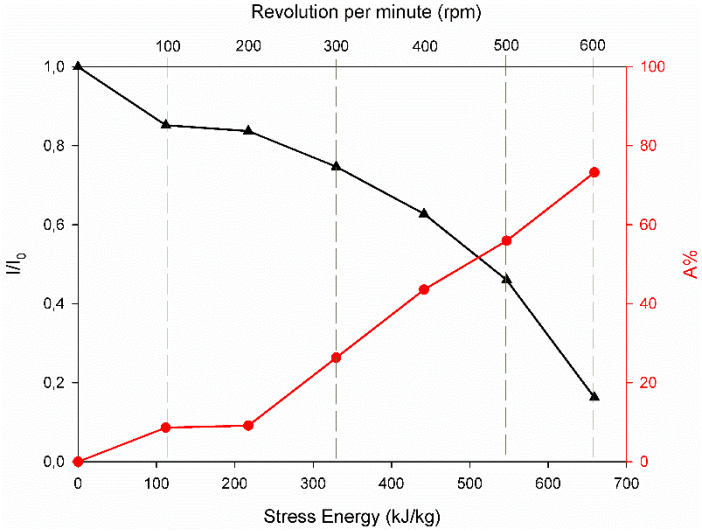

Figure 3. Stress Energy-I/I_0 and Stress Energy-%A dependance according to rpm

Effect of ball-to-mass ratio was given in Figure 4. Determination of ball-to-mass ratio was conducted at 600 rpm for 30 min. Tincalconite formation was observed for all parameter. At Figure 5, increased ball-to-mass ratio caused increment in stress energy and amorphization degree. Additionally, peak rate decrement occurred.

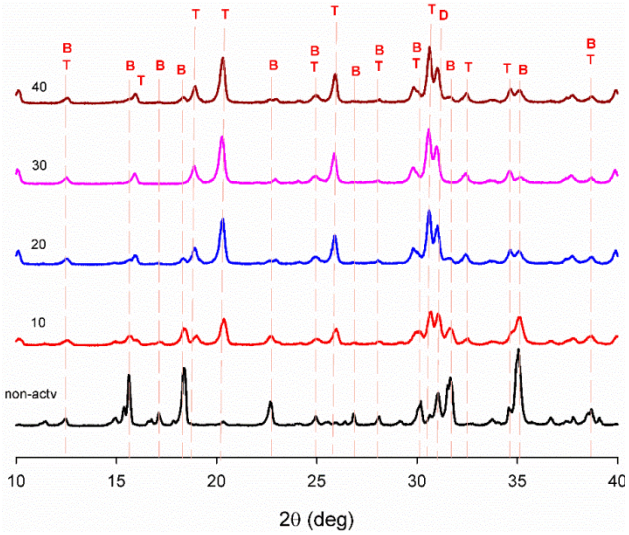

Figure 4. X-ray diffraction analysis of mechanically activated tincal at different ball-to-mass ratios.

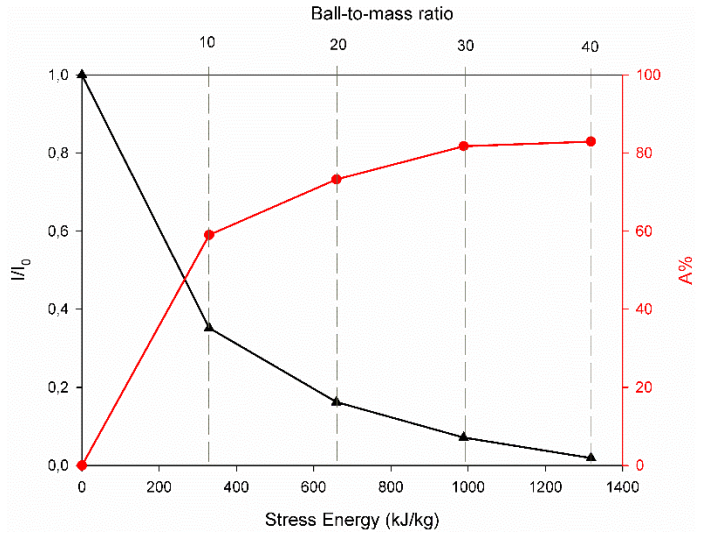

Figure 5. Stress Energy-I/I_0 and Stress Energy-%A dependance according to ball-to-mass ratio

When sample mass and amorphization degree considered together with regards to industrial application, higher ball-to-mass ratio like 30 and 40 not be logical for small variance in amorphization degree as shown in Figure 5 due to the less feed. Taking into consideration of this situation, ball-to-mass ratio was fixed at 20 for mechanical activation duration studies.

Role of mechanical activation duration was given in Figure 6. After 15 min, borax patterns lost substantially and tincalconite formation occurred. Prolonged mechanical activation time caused shifting and/or broadening of the peaks caused from mechanism of mechanical activation that base on motion of milling equipment and taken place impact on the particulate system. One of the effects of mechanical activation is released heat from the friction of the ball-sample-bowl at 600 rpm could be caused partial decomposition of tincalconite. It is stated that for a planetary mill, typical temperature is over 200°C and during milling two kinds of temperature are considered: local temperature pulses due to ball collisions and overall temperature in the vial (Baláž et al., 2013).

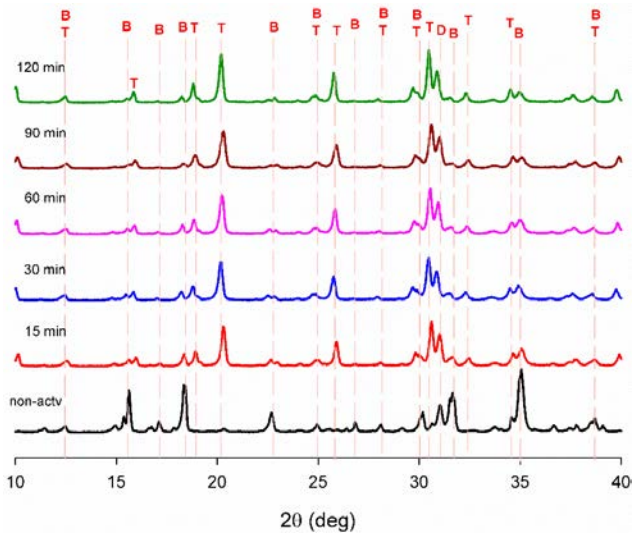

Figure 6. X-ray diffraction analysis of mechanically activated tincal for different durations.

Tromans and Meech (2001) stated that line broadening and disappearance of diffraction peaks that taken place on X-ray patterns after extended milling is a result of formation of meta-stable -amorphous phase- related with alteration of long-range lattice periodicity because of large number of dislocations and their related strain fields.

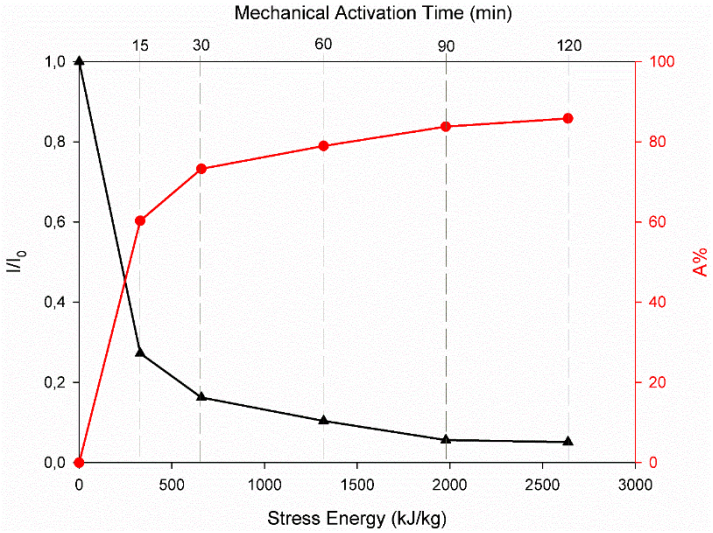

Figure 7. Stress Energy-I/I0 and Stress Energy-%A dependence according to ball-to-mass ratio

When Figure 7 was examined, it was understood that after 15 min mechanical activation duration, peak rate was drastically decreased with increased stress energy. More stress energy than provided stress energy about 360 kJ/kg by 15 min mechanical activation, formed little change in the intensity of the diffraction pattern and

amorphization degree. This phenomenon means that both crystal structure and crystal size didn't affect from increased mechanical activation time anymore after 15 min.

FT-IR analysis of non-activated and activated for 15 and 60 min samples are given in Figure 8. The region of 2700-3700 cm^{-1} is attributed as hydroxyl stretching region (Ruan et al., 2002). 3344 cm^{-1}, 3498 cm^{-1} and 3576 cm^{-1} band centres were determined in this region. But for mechanical activated samples band centres were determined at 3008 cm^{-1}, 3348 cm^{-1} and 3502 cm^{-1}. 3576 cm^{-1} was absent for these samples.

A shift of band centre to higher position means that strength of bonds is decreased. If the band shifts to a lower position it will result in tighter bonding. This region that indicates O-H stretching vibration is sensitive to dehydroxylation temperature. It was used for dehydroxylation of goethite by Ruan et al., (2002).

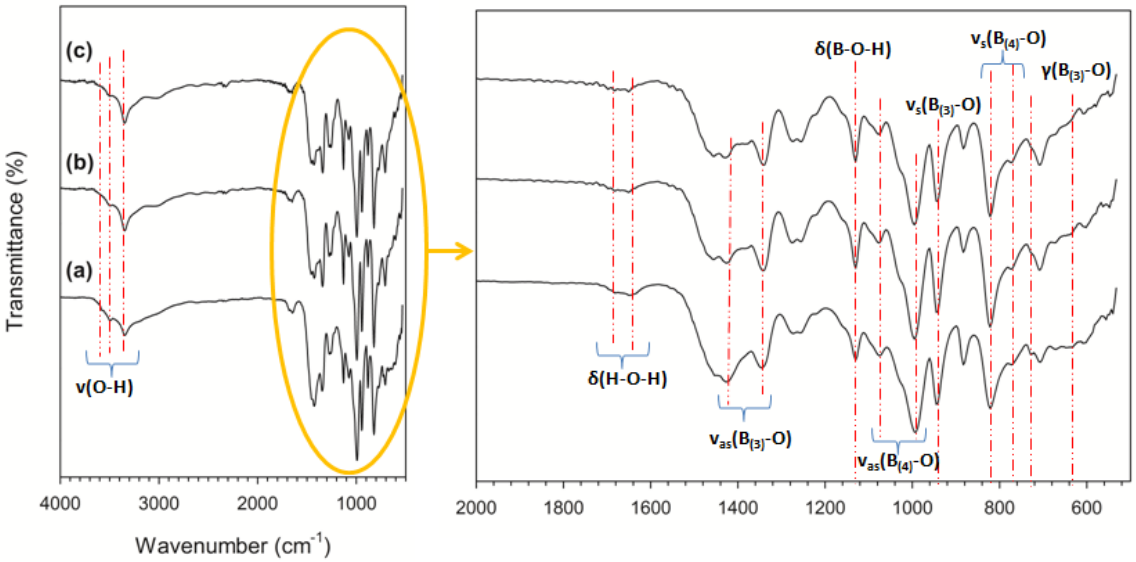

Figure 8. FT-IR analysis of a) non-activated and activated for b) 15 min and c) 60 min samples.

From these results, it can be said that with mechanical activation dehydroxylation was partially started but not completed because of existence of the characteristic band that differ in transmittance and broadness than the non-activated. The FT-IR analysis of ulexite that used for sodium borohydride production by Piskin (2009) had a band that found at 1625.84 cm^{-1} clarified as a free H_2O band. Yan et al. (2001) stated that sample at 70°C, the H-O-H bending mode exist at 1636 cm^{-1} and 1691 cm^{-1}. Like these studies, H-O-H bending mode was varied between 1578 cm^{-1} and 1691 cm^{-1} for different studies (Yan et al., 2001; Zhihong et al., 2003; Liu et al., 2006; Figen et al., 2010; Wang et al., 2010; Goel et al., 2013). Figen et al. (2010) and Wang et al. (2010) also stated that the H-O-H bending modes for their studies that found 1691-1649 cm^{-1} and 1662 cm^{-1} respectively, showed that the sample contains crystal water molecules. For tincal sample, this band was determined at 1647 cm^{-1} and 1681 cm^{-1}, and for activated sample they positioned at 1651 cm^{-1} and 1681 cm^{-1} that means mechanically activated samples still contain crystal water but not same strength of initial bond. In our FT-IR analysis wavenumber of the peaks are matching with data of Jun et al. (1995) for FT-IR of tetraborates. 730 cm^{-1} is clarified as in plane bending mode of CO_3 (Ji et al., 2009). As stated in the XRD results, tincal samples contain dolomite and this band confirms the presence of dolomite. But in mechanically activated samples this band couldn't determine.

DTA-TG analysis of the samples is given in Figure 9 and Figure 10 respectively. Tincal is an ore that starts losing its water at approximately 330K (Ekmekyapar et al., 1997). Non- activated and activated samples were compared in terms of physical water loss, peak temperatures of 70°C and 40°C were determined for non-activated and activated for 15 min samples. No related reaction at this temperature interval was determined for 60 min activated sample. Second and third endothermic reaction peak temperatures were determined at 115°C and 135°C for non-activated sample. This gradual decomposition trend turned into one step for 15 min mechanically activated sample at 140°C. 125°C and 135°C peak temperatures were determined for 60 min sample.

From the DTA analysis it was understood that for non-activated, activated for 15 and 60 min samples, tincalconite formation finished at 135°C. But the advantage of mechanical activation was confirmed as endothermic peaks area that is a describer of energy requirement of a reaction (Tunç et al., 2014).

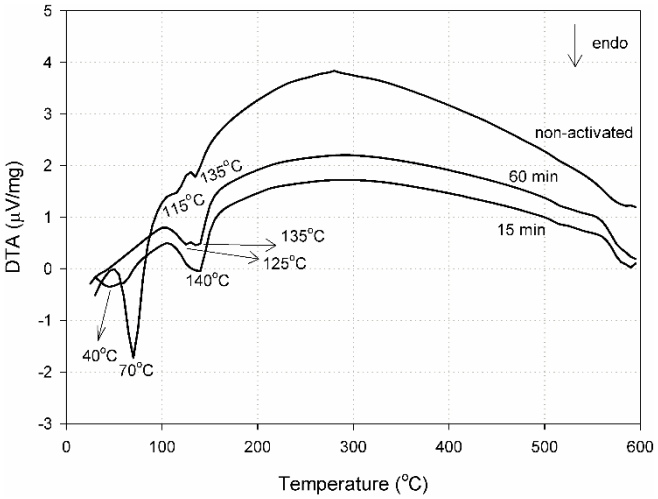

Figure 9. DTA analysis of non-activated and activated for 15 min and 60 min tincal.

When Figure 10 was examined it was understood that for non-activated sample, mass loss started as heating but for activated one, because of the physical water loss occurred during milling, decomposition started when reached at a certain temperature. When mass loss was investigated, this occurrent supported the heat occurrence during milling that cause elimination of water from the structure. Mass losses were calculated as 43%, %33 and %32 for non-activated, activated for 15 and 60 min activated samples. Form the XRD and DTA results it was understood that, decomposition of sample started in the milling process and TG results supported this phenomenon. Mass losses of the activated samples were less than the original one.

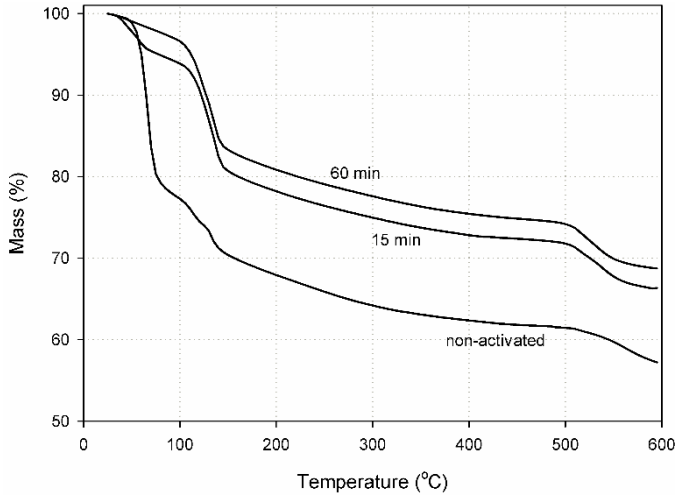

Figure 10. TG analysis of non-activated and activated for 15 min and 60 min tincal.

As determined from the XRD results, after 15 min mechanical activation, most of the diffraction peaks correspond to tincalconite and stress energy-I/I_0 graph showed that there was no need to excess energy input after 15 min to effect borax structure.

Conclusion

Tincal that is the raw material of the borax production was mechanically activated for observing structural alterations and structural water behaviour. Speed of main disc, ball-to-mass ratio and duration were chosen as parameters for mechanical activation process. In hydrated minerals, excess water molecules may be a problem during storage, transportation and production of other related boron products in the meaning of energy consumption.

XRD results shows that original tincal sample consist of borax and dolomite crystals.

By increasing the speed of main disc because of the friction thereby occurred heat energy, borax was decomposed and tincalconite formation occurred.
For industrial application, higher ball-to-mass ratio like 30 and 40 not be logical for little variance in amorphization degree due to the less feed. Taking into consideration of this situation, ball-to-mass ratio was fixed at 20 for mechanical activation duration studies.

Mechanical activation duration studies showed that after 15 min mechanical activation procedure, crystal structure changes about 75% by means of amorphization. Provided heat during mechanical activation via milling media motion, impact and friction cause in situ phase transformation of borax decahydrate to borax pentahydrate (tincalconite). More stress energy than provided stress energy about 360 kJ/kg by 15 min mechanical activation formed little change in the intensity of the diffraction pattern. This phenomenon means that both crystal structure and crystal size didn't affect from increased mechanical activation time anymore after 15 min and DTA-TG results supported this finding.

Borax decahydrate to borax pentahydrate (tincalconite) transformation was supported by FT-IR analysis. Because of the two molecules of water as hydroxyl unit in the borate ion, hydroxyl stretching vibrations were still present but not positioned at the same wavenumber that means amorphization by mechanical activation in force about alteration of the structure via changing the bond strength.

So, it can be said that, by mechanical activation tincal structure was changed and water lost was achieved without having to heat treatment.

References

Alves, A. K., Bergmann, C. P., Berutti, F. A. (2013). *Novel Synthesis and Characterization of Nanostructured Materials*, Verlag Berlin Heidelberg: Springer.

Baláž, P., Achimovičová, M., Baláž, M., Billik, P., Cherkezova-Zheleva, Z., Criado, J. M., Delogu, F., Dutková, E., Gaffet, E., Gotor, F. J., Kumar, R., Mitov, I., Rojac, T., Senna, M., Streletskii, A., Wieczorek-Ciurowa, K. (2013). Hallmarks of mechanochemistry: from nanoparticles to technology. *Chem. Soc. Rev.*, 42 (pp.7571-7637).

Baláž, P. (2008). *Mechanochemistry in Nanoscience and Minerals Engineering*, Berlin, Springer-Verlag.

Boncukcuoğlu, R., Kocakerim, M. M., Erşahan, H. (1999). Upgrading of the reactor waste obtained during borax production from tincal. *Minerals Engineering*, 12 (pp.1275-1280).

Ekmekyapar, A., Baysar, A., and Künkül, A. (1997). Dehydration kinetics of tincal and borax by thermal analysis. *Ind. Eng. Chem. Res.*, 36 (pp.3487-3490).

Erdemoğlu, M., Aydoğan, A., Gock, E. (2009). Effects of intensive grinding on the dissolution of celestite in acidic chloride medium. *Minerals Engineering*, 22 (14-24).

Figen, A. K., Yılmaz, M. S., Pişkin, S. (2010). Structural characterization and dehydration kinetics of Kırka inderite mineral: Application of non-isothermal models. *Materials Characterization*, 61 (pp.640-647).

Goel, N., Sinha, N., Kumar, B. (2013). Growth and properties of sodium tetraborate decahydrate single crystals. *Materials Research Bulletin* 48 (pp.1632–1636).

Ji, J., Ge, Y., Balsam, W., Damuth, J. E., Chen, J. (2009). Rapid identification of dolomite using a Fourier Transform Infrared Spectrophotometer (FTIR): A fast method for identifying Heinrich events in IODP Site U1308. *Marine Geology*, 258 (pp.60–68).

Jun, L., Shuping, X., Shiyang, G. (1995). FT-IR and Raman spectroscopic study of hydrated borates. *Spectrochimica Acta Part A: Molecular and Biomolecular Spectroscopy*, 51 (pp.519-532).

Kavas, T., Christogerou, A., Pontikes, Y., Angelopoulos, G.N. (2011). Valorisation of different types of boron-containing wastes for the production of lightweight aggregates. *Journal of Hazardous Materials*, 185 (pp.1381–1389).

Koçakuşak, S., Köroğlu, J. H., Ekinci, E., Tolun, R. (1995). Production of anhydrous borax using microwave heating. *Ind. Eng. Chem. Res.*, 34 (pp. 881-885).

Liu, Z., Li, P. and Zuo, C. (2006). Standard molar enthalpies of formation for the two hydrated calcium borates $xCaO.5B_2O_3.yH_2O$ (x = 2 and 4, y = 5 and 7). *J. Chem. Eng. Data*, 51 (pp. 272-275).

Liu, J., Xi, J., Yang, W., Hu, Y., Zhang, Y., Wang, Y., Zhou, J. (2014). Effect of magnesium on the burning characteristics of boron particles. *Acta Astronautica*, 96 (pp. 89-96).

Piskin, M. B. (2009). Investigation of sodium borohydride production process: Ulexite mineral as a boron source. *International Journal of Hydrogen Energy*, 34 (pp. 4773-4779).

Ruan, H. D., Frost, R. L., Kloprogge, J. T. and Duong, L. (2002). Infrared spectroscopy of goethite dehydroxylation. II. Effect of aluminium substitution on the behaviour of hydroxyl units. *Spectrochimica Acta Part A: Molecular and Biomolecular Spectroscopy*, 58 (pp. 479-491).

Sahin, O., Bulutcu, A. N. (2002). Production of high bulk density anhydrous borax in fluidized bed granulator. *Chemical Engineering and Processing: Process Intensification*, 41 (pp. 135–141).

Tromans, D., Meech, J. A. (2001). Enhanced dissolution of minerals: stored energy, amorphism and mechanical activation. *Minerals Engineering*, 14 (pp. 1359-1377).

Tunç, T., Apaydin, F., Yildiz, K. (2014). Structural alterations and thermal behaviour of mechanically activated alunite ore. *J Therm Anal Calorim.*, 118 (pp. 883-889).

Wang, Y., Pan, S., Hou, X., Liu, G., Wang, J., Jia, D. (2010). Non-centrosymmetric sodium borate: Crystal growth, characterization and properties on $Na_2B_4O_{12}H_{10}$. *Solid State Sciences*, 12 (pp. 1726-1730)

Yan, J., Yongzhong, J., Shiyang, G., Haidong, W., Shiying, Y. (2001). Thermal decomposition of $K_2O.CaO.4B_2O_3.12H_2O$. *Thermochimica Acta*, 374 (pp. 51-54).

Zhang, D.L. (2004). Processing of advanced materials using high-energy mechanical milling. *Progress in Materials Science*, 49 (pp. 537–560).

Zhihong, L., Bo, G., Mancheng, H., Shuni, L., Shuping, X. (2003). FT-IR and Raman spectroscopic analysis of hydrated cesium borates and their saturated aqueous solution. *Spectrochimica Acta Part A: Molecular and Biomolecular Spectroscopy*, 59 (pp. 2741-2745).

